Hindawi Publishing Corporation
EURASIP Journal on Wireless Communications and Networking
Volume 2010, Article ID 123674, 13 pages
doi:10.1155/2010/123674

Research Article

Spectrum Sensing for Cognitive Radios with Transmission Statistics: Considering Linear Frequency Sweeping

Sithamparanathan Kandeepan, Radoslaw Piesiewicz, Tuncer C. Aysal, Abdur Rahim Biswas, and Imrich Chlamtac

Create-Net International Research Centre, Cognitive Information Networks (CoIN) Group, Povo 38123, Trento, Italy

Correspondence should be addressed to Sithamparanathan Kandeepan, kandeepan@ieee.org

Received 28 September 2009; Revised 8 January 2010; Accepted 6 March 2010

Academic Editor: Gianluigi Ferrari

The spectrum sensing performance of Cognitive Radios (CRs) considering noisy signal measurements and the time domain transmission statistics of the Primary User (PU) is considered in this paper. When the spectrum is linearly swept in the frequency domain continuously to detect the presence of the PU the time-domain statistics of the PU plays an important role in the detection performance. This is true especially when the PU's bandwidth is much smaller than the CR's scanning frequency range. We model the transmission statistics that is the temporal characteristics of the PU as a Poisson arrival process with a random occupancy time. The spectrum sensing performance at the CR node is then theoretically analyzed based on noisy envelope detection together with the time domain spectral occupancy statistics. The miss detection and false alarm probabilities are derived from the considered spectral occupancy model and the noise model, and we present simulation results to verify our theoretical analysis. We also study the minimum required sensing time for the wideband CR to reliably detect the narrowband PU with a given confidence level considering its temporal characteristics.

1. Introduction

The Cognitive Radio (CR) concept is being under deep consideration to opportunistically utilize the electromagnetic spectrum for efficient radio transmission [1–4]. The CR basically acts as a secondary user of the spectrum allowing the incumbent (primary) users of the spectrum to have higher priority for spectrum utilization. The notion of efficient spectrum utilization has also attracted the radio spectrum regulatory bodies around the world [5, 6] to further investigate the technology. The secondary users therefore need to learn the environment in the presence of any primary users (PUs) and keep track of them to ensure that it does not interfere with the PU. Learning the environment and performing radio scene analysis (RSA) becomes a challenging and an essential task for the CR to successfully perform secondary communication with reduced interference to the PU. Reliably performing the RSA is quite important in order to avoid interfering with the PU's communications and also to satisfy the regulatory requirements. To perform such an RSA, the CR nodes need to sense the spectrum continuously in the time, frequency, and spatial domains. Spectrum sensing therefore, amongst many, is one of the key functionalities of a CR in order to perform (RSA) of the communication environment.

1.1. Problem Statement. In the recent years, Ultra Wideband (UWB) technology has emerged as one of the key candidates for CR based secondary user communications [7, 8]. When UWB technology is used as CRs for secondary communications, it is required to scan the entire spectrum from 2.9 GHz–10 GHz (in many cases a significant portion of it) to detect the presence of any PUs in the network. In such situations, scanning a wide range of frequencies (7 GHz) can be a time consuming process and hence a narrow band PU, which has a bandwidth much smaller than the UWB node, can be gone undetected when the UWB-CR node is scanning a large portion of the spectrum. It is obvious to state that such miss detection depends on the PU's transmission statistics, or in other words the Spectral occupancy Statistics

(SoS) as well as the spectrum sniffing hardware unit of the UWB-CR node and the corresponding time required to sense the spectrum. Such a problem is considered to be a crucial one to be solved by many researchers and engineers working in this filed, such as in the European Union funded 20 M-Euros project on EUWB [8]. The problem defined here is not specific to UWB based CR systems only, but in general it applies to any CR systems with a bandwidth much larger than the bandwidth of the potential victim services (i.e., the PUs) in the network.

1.2. Literature Review. Spectrum sensing techniques have been heavily discussed and treated in the literature and one could refer to [3, 4, 9–28] for further reading. The performance of different spectrum sensing techniques are measured in terms of the probability of false alarm and the probability of miss detection for noisy sensing. In our work however, in addition to noisy sensing, we also include the SoS (i.e., the temporal characteristics) of the PU and analyze the detection performance of the CR nodes for wideband sensing. In order to perform theoretical analysis some mathematical models should be followed for the temporal characteristics of the PU. The Poisson model for the arrival process is the most common model used in the research literature for theoretical derivations and performance analysis [29–40], and also recommended in the International Telecommunication Union's (ITU) handbook on Teletraffic Engineering [32]. Moreover, Poisson models are also verified for several cases [34–40], especially for the Internet traffic when the load is higher [34]. Therefore, we adopt such a model in our work. It should be noted that there also exist empirical models for various traffic sources [29, 30, 30, 31, 31–44] and for various radio access technologies mostly derived from the Poisson arrival process.

Furthermore, the authors in [21] have used the Poisson traffic model to design an admission controller for the CR node to improve the Quality of Service (QoS) for secondary transmissions. In [22], for Poisson based PU traffic, the authors have studied by means of simulations the trade-off between sensing time and the achievable throughput by considering the probability of collision. The Poisson traffic model is also used in [23, 24] to derive a-*priori* probability based detection schemes for spectrum sensing and have presented some numerical results on the improvement over the traditional energy-based detection [45] and the classical Maximum Likelihood- (ML-) based detection techniques [46], respectively. A channel selection scheme for CR nodes for a multichannel multiuser environment is also proposed-based on Poisson traffic model in [25], and recently in [26, 27] we have studied the performance of shared spectrums sensing for UWB-based CR assuming the Poisson model for the PU. Furthermore, moving away from the Poisson based theoretical model, the authors in [47] have analyzed the performances of dynamic spectrum access techniques based on experimentally measured spectrum occupancy statistics.

1.3. Contribution. In this paper, we study the performance of detecting the PU based on its time domain SoS, by classifying them as light, average or heavy users of the spectrum, together with noisy sensing at the CR nodes. We mainly consider the case where the PU bandwidth is much smaller than the CR's spectrum scanning frequency range. Though the references in [22–26] have considered the Poisson model for the PU channel SoS they have presented mainly some simulation results to analyze the performances of the the CR node for spectrum sensing and channel occupancy efficiency. In our work presented here, we perform some detailed theoretical analysis of the performance of PU detection, based on an envelope-based energy detector, by initially considering the transmission statistics only case and then together with the sensing noise. The theoretical anaylses are also verified by simulations. We also study the minimum required sensing time for the CR node to reliably detect the narrow band PU given its temporal characteristics.

1.4. Paper Organization. The rest of the paper is organized as follows. In Section 2, we provide the model for the CR network, and in Section 3, we derive the Poisson arrival model for the PU's transmission statistics from the fundamentals. In Section 4, we provide the signal envelope based spectrum sensing technique followed by some theoretical analysis on the detection performances for the noiseless case with a constant channel occupancy (hold) time in Section 5. In Section 6, we present a PU detection risk analysis based on the transmission statistics (Poisson process) of the PU. In Section 7, we present the detection performance considering noise, and in Section 8, we extend the analysis for a random channel occupancy (hold) time. In Section 9, we present the sensing time requirements for the CR based on the SoS of the PU, and finally we make some concluding remarks in Section 10.

2. Cognitive Radio-System Model

The CR network model is presented in this section. We define the following parameters for the wideband sensing CR nodes and the PU in the network. For the PU, we define B_w as its transmission bandwidth, Δ as the time duration between transmissions (spectrum idle time) that is calculated from the end to the beginning of two successive transmissions, and τ as the PU's transmission duration (spectrum hold/busy time) per transmission. For the CR node, we define W as the total observation bandwidth to sweep, and T_w as the total time to *linearly* sweep the observation bandwidth W. Linear sweeping is defined by having some constant rate for sweeping the frequency, or in other words the time to sweep a range of frequencies is proportional to the same range of frequencies. Figure 1 depicts the above parameters and also shows the frequency-time observation plot which explains the spectrum scanning process of the wideband sensing CR node. As depicted in the figure, the cognitive radio scans the entire spectrum linearly at a rate of W/T_w. Using such a linear frequency sweeping process, given that the PU is transmitting, the CR node can only detect the PU during its mth scan within the time slot (only) from $t_1^m = t_0 + f_1 T_w/W + (m-1)T_w$ and $t_2^m = t_0 + f_2 T_w/W + (m-1)T_w$, where t_0 is an arbitrary real constant, f_1 and f_2 are the edge frequencies of the transmission bandwidth of the PU with $m = 1, 2, \ldots,$

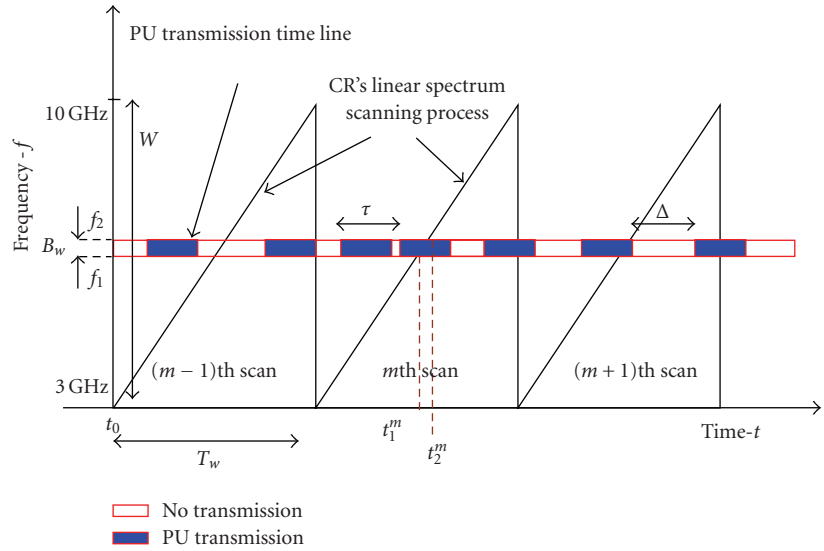

Figure 1: Linear ultra wideband spectrum scanning process for detecting a narrow band primary user: The frequency versus time plot.

and $f_1 < f_2$. Below, we summarize the abovementioned parameters:

(i) B_w—PU transmission bandwidth,

(ii) Δ, τ—time duration between successive transmissions, and the time duration of transmission of the PU, respectively,

(iii) f_1, f_2—edge frequencies of the PU transmission bandwidth ($f_1 < f_2$),

(iv) W—total bandwidth to be scanned by the CR node,

(v) T_w—average time to scan the frequency band W by the CR node,

(vi) t_1^m, t_2^m—start and end times of scanning the PU bandwidth by the CR node, as shown in Figure 1, during the mth iteration.

The presence of a PU in the network is defined by the hypotheses H_0 and H_1, as described in (1). Given that the PU is detected during the mth scan, the CR decides upon H_1 for the entire period of the scan before reinitializing it back to H_0 for the successive scan (i.e., $(m+1)$th scan). The hypothetical decision d_m made by the CR node at the end of every scan for the particular PU within the frequency band of f_1 and f_2 in the absence of noise can be mathematically defined as follows:

$$d_m = \begin{cases} 0, & H_0 \quad \text{CR does not detect any} \\ & \quad \text{PU transmissions } \forall t \in [t_1^m, t_2^m], \\ 1, & H_1 \quad \text{CR detects a PU transmission} \\ & \quad \text{for some } t \in [t_1^m, t_2^m]. \end{cases} \tag{1}$$

A more generic detection model considering the PU SoS together with the sensing noise at the CR node is provided in Section 4. The PU's transmission is modeled as a Poisson arrival process. Therefore, Δ follows an exponential distribution [30] with a mean time between transmission given by Δ_a. We validate the Poisson arrival model for the CR network that we consider here by referring back to Section 1: Literature Review. In other words, the CR network model considered here has a PU delivering Poissonian traffic to the network within its frequency band. Initially, we treat the transmission duration (hold time) τ of the PU as a constant to simplify the analysis and then in Section 8 we extend the analysis to a random transmission duration τ by modeling it as a random process.

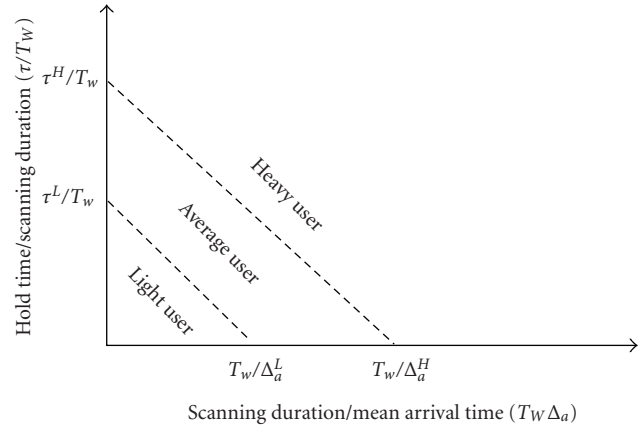

Figure 2: Spectrum occupancy levels of the primary user based on the Poisson arrival process.

Furthermore, based on the values of Δ_a and τ we can characterize the spectral occupancy levels of a PUs as *light*, *average*, or *heavy* users. Figure 2 depicts the spectral occupancy levels of a PU based on their traffic characteristics. In the figure, we further see that the pairs $\{\Delta_a^L, \tau^L\}$ and $\{\Delta_a^H, \tau^H\}$ separate the occupancy level regions of the PUs as *light*, *average*, or *heavy*. Corresponding to the occupancy levels, we also characterize the risk of miss detecting the PU as *High Risk*, *Medium Risk*, and *Low Risk* regions, respectively.

For analytical purposes, the risk regions for miss detecting the PU are defined by

(i) *high risk region (light user)*; for $0 < T_w/\Delta_a < T_w/\Delta_a^L$ and $0 < \tau/T_w < \tau^L/T_w$,

(ii) *medium risk region (average user)*; for $T_w/\Delta_a^L < T_w/\Delta_a < T_w/\Delta_a^H$ and $\tau^L/T_w < \tau/T_w < \tau^H/T_w$,

(iii) *low risk region (heavy user)*; for $T_w/\Delta_a^H < T_w/\Delta_a$ and $\tau^H/T_w < \tau/T_w$.

In later sections, by using the detection probabilities derived from our theoretical analyses, we present numerical values for $\Delta_a^L, \Delta_a^H, \tau^L$, and τ^H.

3. Primary User Spectral Occupancy Statistics

To define the primary user's spectral occupancy statistics based on the Poisson arrival process we state (consider) some axioms. It is important to note that these axioms are the fundamentals in defining the Poisson arrival process in general, and based on these axioms we then analyze the spectrum sensing detection performances considering the spectral occupancy model of the PU. Let $N(t)$ be the number of times that the PU has been present in the network (number of transmissions) up to time t, where $t \in \Re$, the axioms are then defined as in [46].

Axiom 1. At time $t = 0$, the PU has got no occupancy of the spectrum at all. That is, $N(0) = 0$.

Axiom 2. Incremental independency and stationarity of $N(t)$. That is, if $J_1 = N(t_2) - N(t_1)$ and $J_2 = N(t_4) - N(t_3)$ for some $t_1, t_2, t_3, t_4 \in t$ such that $t_1 < t_2 < t_3 < t_4$, then J_1 and J_2 are independent. Further, if $t_4 - t_3 = t_2 - t_1$, then J_1 and J_2 have the same statistical distributions.

The Poisson distribution for the arrival process is then given by

$$P[N(t) = n] = \exp(-\lambda t)\frac{(\lambda t)^n}{n!}, \tag{2}$$

where $n = 0, 1, 2, \ldots$ and $\lambda = 1/\Delta_a$ is the mean arrival (spectral occupancy) rate of the PU. On the other hand, the occupancy time τ of the PU is initially considered to be a constant. Such a model essentially creates an M/D/1 arrival model considering a single CR and single PU system with a Poissonian arrival (M) and a deterministic (D) occupancy time. In later sections, we extend this to an M/M/1 arrival model by considering an exponential distribution and an M/G/1 model considering a Pareto distribution for the random occupancy time for the PU transmissions.

4. Spectrum Sensing

The spectrum sensing technique considered here is the signal envelope-based method [45] where the envelope of the signal is computed within a given range of frequencies in time and compared against a threshold value μ. We consider the envelope-based detection method over the standard energy-based detection method [45, 48–50] mainly considering its simplicity in hardware implementation and computation. From the analytical framework we provide in this paper on the detection performance of the envelope-based detector, together with SoS of the PU, it is rather straight forward to derive the corresponding theoretical expressions for the energy-based detector and perform similar analyses to the ones that we present here. The Energy detectors in general including the envelope-based detector have drawbacks [10, 11, 49] for spectral occupancy detection especially when the noise power is not known, but on the other hand it is the simplest detection method when the CR node has got no knowledge about the PU transmission.

The received baseband signal of bandwidth B_w in its complex envelope form received over a time period of $t_1^m \le t \le t_2^m$ is given by

$$r(t) = \begin{cases} \nu(t), & \text{when PU is not present,} \\ s(t) + \nu(t), & \text{when PU is present,} \end{cases} \tag{3}$$

where, $s(t)$ is the complex envelope of the received signal from the PU without noise, and $\nu(t)$ is the additive bandpass and band limited complex noise component associated with the sensing process. The additive noise $\nu(t)$ is modeled as a zero mean complex Gaussian random process with a power of $2\sigma^2$ over a bandwidth B_w. Note that in (3) we only consider the signal of our interest given within the frequencies f_1 and f_2 (corresponding to the scanning time duration of $t_1^m \le t \le t_2^m$). Since we consider only one PU in our model, therefore $r(t)$ corresponds to the signal received within the PU's transmission bandwidth. We also assume negligible fading associated with $s(t)$ in our model or in other words the amount of fading is small considering the time period for computing the envelope (energy) of the signal, which is a valid assumption as there exist many cases with slow fading scenarios [51]. The envelope of the received signal at $t = \alpha$ over a time of $t_1^m \le \alpha \le t_2^m$ is used as the test statistic $\xi_s(\alpha)$ to detect the PU (transmitting in the frequency band between f_1 and f_2), where $\xi_s(\alpha)$ is given by

$$\xi_s(\alpha) = |r(t)|_{t=\alpha} \quad \text{for } t_1^m \le \alpha \le t_2^m. \tag{4}$$

Further more, we define the signal to noise ratio as $\rho = E_s/2\sigma^2$, where E_s is the power of $s(t)$ over the frequency band of f_1 to f_2 given by

$$E_s = \frac{1}{t_2^m - t_1^m}\int_{t_1^m}^{t_2^m} s(t)\tilde{s}(t)dt, \tag{5}$$

where $\tilde{s}(t)$ denotes the complex conjugate of $s(t)$. The generic detection criteria in deciding whether a PU is present or not for the mth scan, considering the sensing noise as well as the linear spectrum scanning process of the CR, is then given by,

$$d_m = \begin{cases} 0; & H_0 \quad \text{for } \xi_s(t) < \mu, \forall\, t \in [t_1^m, t_2^m], \\ 1; & H_1 \quad \text{for } \xi_s(t) \ge \mu, \text{ for some } t \in [t_1^m, t_2^m]. \end{cases} \tag{6}$$

Note that, as described in (6), we are only interested in the detection of a PU within the spectral range of f_1 to

f_2. The test statistic $\xi_s(\alpha)$ follows two different distributions under the hypotheses H_0 and H_1 depending on whether the signal $s(t)$ is present or not. From the signal model presented in (3), it is well known that [46] (since $\nu(t)$ is complex Gaussian) ξ_s follows a Rayleigh distribution under H_0 and a Rice distribution under H_1, given by

$$f_{\xi_s|H_0}(\xi_s) = \frac{\xi_s}{\sigma^2}\exp\left(-\frac{\xi_s^2}{2\sigma^2}\right),$$
$$f_{\xi_s|H_1}(\xi_s) = \frac{\xi_s}{\sigma^2}\exp\left(-\frac{(\xi_s^2+E_r^2)}{2\sigma^2}\right)I_0\left(\frac{\xi_s E_r}{\sigma^2}\right) \tag{7}$$

where E_r is the time domain root mean square value of the signal $r(t)$, and I_0 is the zeroth order modified Bessel function of the first kind. The distributions in (7) are used to analyze the detection performance which we present in the subsequent sections.

5. Performance Analysis: Noiseless Sensing

The theoretical performance analysis for detecting the PU is performed in three stages. Initially, we study the detection performance considering only the SoS of the PU with a constant hold time with no sensing noise (i.e., SNR $\rho = \infty$), then we extend the analysis considering the sensing noise, and then we further extend the analysis for random hold time. We also provide simulation results to support our theoretical analysis.

5.1. Theoretical Analysis. In the noiseless case, the detection performance of the CR node is characterized by the SoS of the PU, the bandwidth B_w of the PU, and the total time T_w for the CR node to scan the entire bandwidth W. As mentioned previously, we assume the CR nodes linearly scan the frequency in time over the desired (wideband) spectrum.

5.1.1. Occupancy Probability. For the PU, we define the spectral occupancy probability P_O as the probability of initiation of at least one transmission by the PU over a time of T_o seconds. Therefore; P_O is given by $P_O = P[N(t = T_o) \geq 1;\ \forall T_o > 0]$. From (2), we find a closed form expression for the probability of occupancy as

$$P_O = 1 - \exp(-\lambda T_o). \tag{8}$$

From (8), we can compute the spectral occupancy probability of the PU for a single scanning period T_w by letting $T_o = T_w$.

5.1.2. Detection Probability. The detection probability, for detecting the PU by the CR node over a single scan duration of T_w, in the noiseless case is defined by the probability of initiation of at least one transmission within the time slot of $t_1^m - \tau \leq t \leq t_2^m$ for the mth scanning iteration (t_1^m and t_2^m are defined in Section 2). The probability of detection is given by $P'_D = P[(N(t_2^m) - N(t_1^m - \tau)) \geq 1]$. Using the *incremental independence and stationarity* property of the arrival process (Axiom 2), we can rewrite P'_D as $P'_D = P[N(\Gamma+\tau) \geq 1]$, where $\Gamma = t_2^m - t_1^m = T_w(f_2 - f_1)/W$, and from (2) we find a closed form expression given by

$$P'_D = 1 - \exp(-\lambda(\tau + \Gamma)). \tag{9}$$

Note that when $\tau + \Gamma = T_w$, then $P'_D = P_O$. Therefore, the CR detects all the transmissions from the PU in a single scanning period. At the same time, we also observe from (9) that $P'_D = 1$ when $\lambda \to \infty$.

5.1.3. Miss Detection Probability. The probability of miss detection is defined by the probability that CR deciding H_0 gives H_1 for a single scan. In other words, miss detection for the noiseless case occurs when there is at least one initiation of transmission occurring for some t outside the interval $t \notin [t_1^m - \tau, t_2^m]$, but no initiations (of transmissions) during the interval, in a single scan. Therefore, for a single scan the miss detection probability is given by

$$P'_M = P\left[(N(t_2^m) - N(t_1^m - \tau)) = 0 \mid (N(\alpha_1) - N(\alpha_2)) \geq 1\right] \tag{10}$$

for some $\alpha_1, \alpha_2 \in [t_0 + mT_w, t_0 + (m+1)T_w]$ and, $\alpha_1, \alpha_2 \notin [t_1^m - \tau, t_2^m]$, with $\alpha_1 > \alpha_2$. Since, the events occuring at $t \in [t_1^m - \tau, t_2^m]$ and $t \notin [t_1^m - \tau, t_2^m]$ in (10) are mutually disjoint, P'_M can be rewritten as $P'_M = P[N(t_2^m) - N(t_1^m - \tau) = 0]$. Again, using the *incremental independence and stationarity* property of the arrival process with (2), we find a closed form expression as

$$P'_M = \exp(-\lambda(\tau + \Gamma)). \tag{11}$$

We further verify the analytical expressions for P'_D and P'_M, from (9) and (11), since $P'_D = 1 - P'_M$.

5.1.4. False Alarm Probability. The false alarm probability for the noiseless case is defined by the probability of detecting a transmission given that no transmissions have been initiated by the PU during a single scan. Since we do not consider noise in this case, the probability of false alarm is simply zero. Further, we could verify this by expressing the false alarm probability as

$$P'_F = P\left[(N(t_2^m) - N(t_1^m - \tau)) \geq 1 \mid (N(t_0 + (m+1)T_w) - N(t_0 + mT_w))\right] = 0, \tag{12}$$

and since $(N(t_0 + (m+1)T_w) - N(t_0 + mT_w)) = 0$ implies that $(N(t_2^m) - N(t_1^m - \tau)) = 0$, giving us $\{((N(t_2^m) - N(t_1^m - \tau)) \geq 1\} \cap \{(N(t_0 + (m+1)T_w) - N(t_0 + mT_w)) = 0\} = \varnothing$, the probability of false alarm for the noiseless case becomes

$$P'_F = 0. \tag{13}$$

5.2. Numerical Results. We present the simulation results in this section using Matlab to verify the theoretical analysis performed in Section 5.1 Simulations were performed using Monte-Carlo techniques to generate the random (Poisson based) PU's transmissions. In our simulations, the Poissonian arrivals are generated using the Binomial

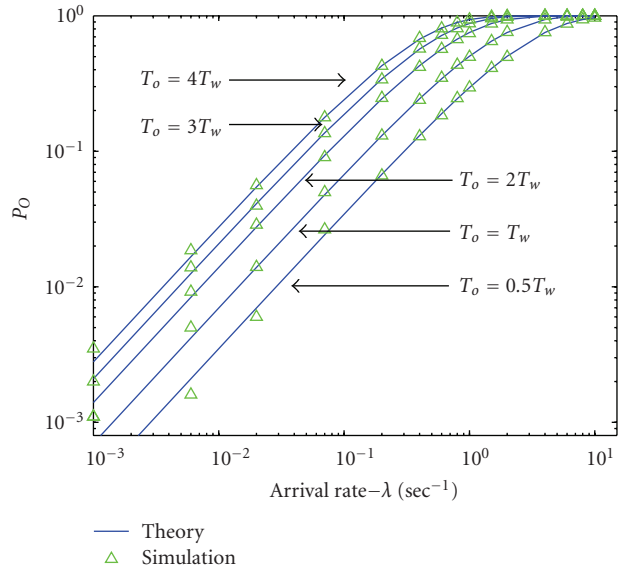

Figure 3: Occupancy probability of the PU versus the arrival rate λ for the Poisson arrival model for various time durations T_o, with $T_w = 0.7$ sec.

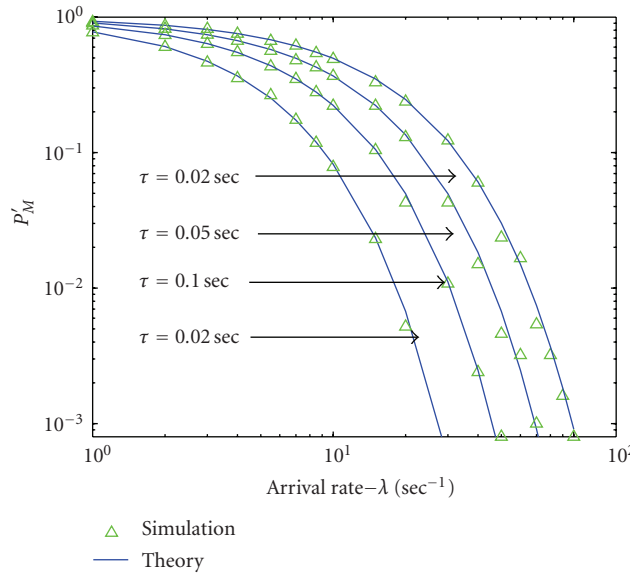

Figure 4: Probability of miss detection for the noiseless case with $T_w = 1$ sec, $B_w = 500$ MHz, $W = 7$ GHz.

counting process by generating a binary random event with a probability of p within a small time duration of T_s, as described in [46, Section 21.3], which converges to a Poissonian process as $T_s \to 0$ with $\lambda = p/T_s$. Simulations were performed in Matlab to generate the random arrival process with a deterministic hold time. Figure 3 presents the occupancy probability P_O for various time durations T_o. From the figure, we observe that P_O increases with the arrival rate λ, as expected, and also marginally improves with the time duration T_o. The figure shows how the the spectral occupancy probability of the PU (defined over a period of $T_o = T_w$) increases when the scanning duration T_w increases for a given arrival rate λ. This observation is quite important, especially when we study the minimum time requirement (minimum T_w) for sensing the PU, which we present in the later sections. Figure 4 depicts the miss detection probability P'_M for various holding times τ and arrival rate λ. From the figures, we see that the detection performance at the CR node improves when both τ and λ increase, we further observe that the improvement in the detection performance is greater when λ increases than when τ increases, relatively. From the figure we also see a very close match between the theoretical expressions derived in the previous section and the simulated results further verifying our analysis.

6. Analysis of the Primary User Miss Detection Risk Regions

In this section, we study the risk regions associated with miss detecting the PU depending on their SoS. Continuing from Section 2 and referring back to Figure 2, here we define the risk regions based on the probability of detection P'_D (for the noiseless case). In other words, we define the values for

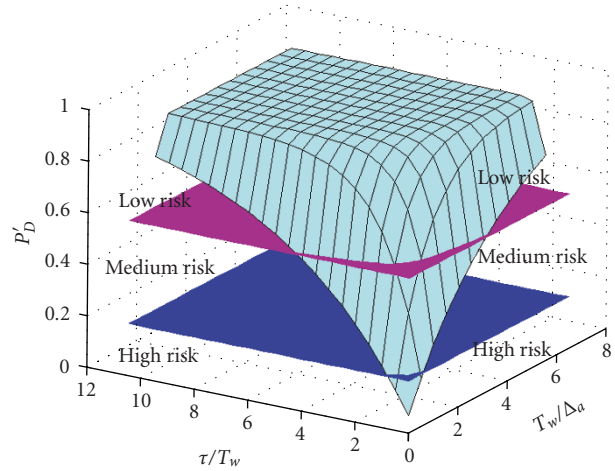

Figure 5: Probability of detection for the noiseless case with $T_w = 1$ sec, $B_w = 500$ MHz, $W = 7$ GHz.

$\tau^L, \tau^H, \Delta_a^L$ and Δ_a^H based on the value of P'_D. Let us define two values for P'_D, given by P'_{D^L} and P'_{D^H}. We define the

(i) *High Risk Region* as the range of values for τ and Δ_a, for all values of P'_D such that $P'_D < P'_{D^L}$,

(ii) *Medium Risk Region* as the range of values for τ and Δ_a such that $P'_{D^L} < P'_D < P'_{D^H}$,

(iii) *Low Risk Region* as the range of values for τ and Δ_a such that $P'_D < P'_{D^H}$.

Figure 5 shows the risk regions of miss detecting the PU by depicting a three-dimensional plot of P'_D for $P'_{D^L} = 0.2$ and $P'_{D^H} = 0.6$ with respect to Δ_a and τ (for the noiseless case). The figure also shows the risk regions separated by two planes given by $P'_{D^L} = 0.2$ and $P'_{D^H} = 0.6$ that define the boundaries of the risk regions. The values of P'_{D^L} and P'_{D^H}

can be varied depending on our traffic model (traffic sources) based on the application.

The values of P'_{D^L} and P'_{D^H} for the risk regions are basically custom defined and chosen to comply with regulatory requirements. For example, if the regulatory requirement for a minimum detection probability (to minimize interference to the PU) is given, then it could be assigned to P'_{D^H}. This would ensure that the low risk region (defined by P'_{D^H}) does satisfy the regulatory requirements, which we explain in Example 1 later. On the other hand, P'_{D^L} which defines the medium and high risk regions is defined by the CR Network as a benchmark for classifying interference level as medium or high interference, respectively, (i.e., interference from the CR to the PU and vice versa).

Further, for a given set of values B_w, T_w and W, we can define two theoretical curves R_1 and R_2 for the boundaries of risk regions, which are given by

$$\begin{aligned} R_1 &: \ln\left(1 - P'_{D^L}\right) + \lambda\Gamma + \lambda\tau = 0, \\ R_2 &: \ln\left(1 - P'_{D^H}\right) + \lambda\Gamma + \lambda\tau = 0, \end{aligned} \tag{14}$$

where $\Gamma = T_w B_w / W$ (from Section 5.1). The curves R_1 and R_2 and the corresponding risk regions are shown in Figure 6. The figure here (Figure 6) defines the risk regions more precisely than Figure 2. Note that the risk regions can be custom defined based on the values of P'_{D^L} and P'_{D^H} that define the curves R_1 and R_2, respectively. As observed in the figure, the risk regions become independent of the hold time τ for small values of τ. In practice, this is true since the detection performance only depends on the arrival rate $\lambda(= 1/\Delta_a)$ for small values of τ/Δ_a. The values of Δ_a^L and Δ_a^H defining the risk regions are then computed from R_1 and R_2, respectively as

$$\begin{aligned} \Delta_a^L &= \lim_{\tau \to 0} R_1 = -\frac{\Gamma}{\ln\left(1 - P'_{D^L}\right)}, \\ \Delta_a^H &= \lim_{\tau \to 0} R_2 = -\frac{\Gamma}{\ln\left(1 - P'_{D^H}\right)}. \end{aligned} \tag{15}$$

For the parameters given in Figure 6, the values of Δ_a defining the risk regions are given by $\Delta_a^L = 0.0064$ sec (for 20% confidence, i.e., $P'_{D^L} = 0.2$) and $\Delta_a^H = 0.0016$ sec (for 60% confidence, i.e., for $P'_{D^H} = 0.6$). The values τ^L and τ^H, on the other hand, can only be defined for a given value of λ, letting $\lambda \to 0$ to compute τ^L and τ^H has no practical significance since when $\lambda = 0$ there are no transmissions from the PU. Therefore, for a given λ, say $\lambda = (1/\Delta_a) = 1/10^{-3}$, we find the values of τ defining the risk regions by using R_1 and R_2 (or by using Figure 6), as $\tau^L = 223.14$ sec and $\tau^H = 916.3$ sec.

Example 1 (WiMedia-UWB based Cognitive Radio System with Constant Scanning Time (T_w)). We now provide an example of a WiMedia based Ultra-Wideband (UWB) [7] CR system which requires a 90% confidence ($P'_D > 0.9, P'_{D^L} = P'_{D^H} = 0.9$) in detecting a PU in the network. The PU system that we consider here is the WiMax radio [52] operating at 3.5 GHz with a bandwidth of $B_w = 10$ MHz and a transmission statistics derived by the Poisson process (Note: In practice the temporal behavior of WiMax transmissions may not be Poisson arrival process, however we consider the Poisson arrival here for analytical purposes). We analyze, for the noiseless case, the values of Δ_a that enables the WiMedia based CR node to detect a WiMax PU with the given confidence level (90%). We assume that the WiMedia system has an operational bandwidth of $W = 1.5$ GHz (from 3 GHz–4.5 GHz) and a hardware that has a spectrum scanning time of $T_W = 10$ msec (assumption only). Then, by using (15), we compute the value of Δ_a for small values of τ, that defines whether the requirement of 90% confidence for detecting the WiMax radio can be achieved or not in the noiseless case. Accordingly, we get $\Delta_a = 2.89 \times 10^{-5}$ where $\Gamma = (10 \times 10^{-3})(10 \times 10^6)/(1.5 \times 10^9) = 6.67 \times 10^{-5}$. Therefore, given a fixed value T_w, the CR can detect the PU with 90% confidence for the noiseless case (or for very high received SNR of the PU signal) provided that the SoS of the PU is such that the mean time between transmissions Δ_a satisfies $\Delta_a < 2.89 \times 10^{-5}$ sec for small values of τ.

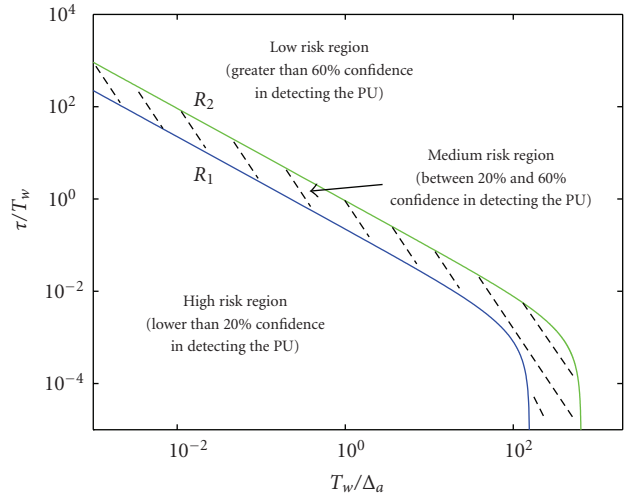

Figure 6: Risk regions associated with PU detection, for $T_w = 1$ sec, $W = 7$ GHz, $B_w = 10$ MHz.

7. Performance Analysis: Noisy Sensing

The detection performance with noise is of great interest to us. In this section, we analyze the overall probability of false alarm and the overall probability of miss detection for the envelope-based PU detection given the Poisson SoS of the PU for noisy sensing.

7.1. Theoretical Analysis. First, we define the four probabilities P_{00}, P_{01}, P_{10}, and P_{11} for the *noiseless case* as, $P_{00} = P[d_m = 0 \mid H_0]$, $P_{01} = P[d_m = 0 \mid H_1]$, $P_{10} = P[d_m = 1 \mid H_0]$, and $P_{11} = P[d_m = 1 \mid H_1]$. From the analysis performed in Section 5, we identify that $P_{00} = 1$, $P_{01} = P'_M$, $P_{10} = P'_F = 0$, and $P_{11} = P'_D$. Then, the overall probability of

detection $P_D = P[\xi_s \geq \mu \mid H_1]$ and the probability of false alarm $P_F = P[\xi_s \geq \mu \mid H_0]$ for the *noisy case* are given by,

$$P_D = f_{\xi_s|H_0}(\xi_s \geq \mu)P_{01} + f_{\xi_s|H_1}(\xi_s \geq \mu)P_{11},$$
$$P_F = f_{\xi_s|H_0}(\xi_s \geq \mu)P_{00} + f_{\xi_s|H_1}(\xi_s \geq \mu)P_{10}. \tag{16}$$

From (16), by using (7), we come up with two closed form expressions for P_D and P_F as

$$P_D = \exp\left(-\frac{\mu^2}{2\sigma^2}\right)P'_M + Q_1\left(\frac{E_r}{\sigma}, \frac{\mu}{\sigma}\right)P'_D,$$
$$P_F = \exp\left(-\frac{\mu^2}{2\sigma^2}\right), \tag{17}$$

where, $Q_1(x_1, x_2)$ is the Marcum Q-Function defined by,

$$Q_1(x_1, x_2) = \int_{x_2}^{\infty} z \exp\left(-\frac{z^2 + x_1^2}{2}\right) I_0(x_1 z)dz. \tag{18}$$

From the expressions we, observe that the probability of false alarm P_F does not depend on the transmission statistics of the PU but only depends on the sensing noise. In the following section, we perform some simulations to study the detection performances and also verify the theoretical analysis performed in this section.

7.2. Complementary Receiver Operating Characteristic Curves and Simulation Results. The Complementary Receiver Operating Characteristic Curves (C-ROCs) for the envelope-based detector is presented here considering the PU transmission statistics. The C-ROC curve is the plot between P_F and P_M by varying the detection threshold μ. Together with the theoretical C-ROC curves, derived from the previous section, we also present some simulation results to verify our theoretical analysis. Monte-Carlo simulations were performed to generate the PU's (Poisson) transmission process and the noisy sensing process with Gaussian noise. Figure 7 shows the C-ROC curves for various SNR values for $\lambda = 25$ and $\tau = 0.01$. As expected, we see that the C-ROC curves improve when the SNR is increased, the figure also shows the probability of miss detection (P'_M) for the noiseless case as well. Figure 8 shows the C-ROC curves for different values of arrival rate λ with $\gamma = 5\,\text{dB}$ and $\tau = 0.02$. From the figure, we observe how the detection performance improves when the arrival rate (spectral occupancy rate) of the PU is increased. Moreover, we see that when λ is increased further the detection performance predominantly depends on the sensing noise. Figure 9 shows the C-ROC curves for various values of spectral hold time τ for $\lambda = 15$ and $\gamma = 5\,\text{dB}$. Improvements in the detection performances are observed when τ is increased but not as much as when λ is increased as in Figure 8. Furthermore, we clearly see that the simulation results very closely match with the theoretical results on all the figures, verifying our analysis in the previous section.

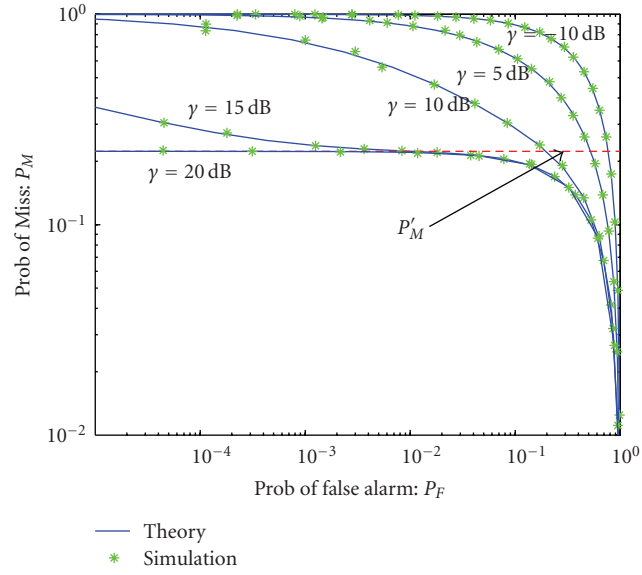

Figure 7: Complementary receiver operating Characteristics curves for various SNR values for the envelope based detector with $W = 7\,\text{GHz}$, $B_w = 500\,\text{MHz}$, $T_w = 0.7\,\text{sec}$, $f_1 = 3.5\,\text{GHz}$, $\lambda = 25\,(\text{sec}^{-1})$, $\tau = 0.01\,\text{sec}$.

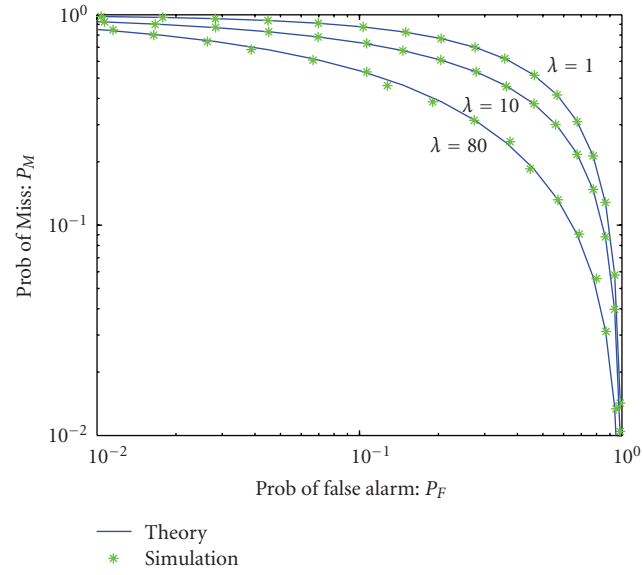

Figure 8: Complementary receiver operating characteristics curves for various arrival rates for the envelope based detector with $W = 7\,\text{GHz}$, $B_w = 500\,\text{MHz}$, $T_w = 0.7\,\text{sec}$, $f_1 = 3.5\,\text{GHz}$, $\gamma = 5\,\text{dB}$, $\tau = 0.02\,\text{sec}$.

8. Performance Analysis: Random Hold Time

In our analysis so far we have assumed a constant hold time τ. In this section we extend the analysis for the detection performance with a randomly distributed hold time τ. We consider two random hold time models namely (1) the exponential distribution which is a traditional way for modeling the call hold time describing many real time applications, and (2) the Pareto distribution which is used to model the World Wide Web IP traffic.

The exponential model is a very traditional model used to describe the random call hold time process. It is useful in modeling voice traffic as recommended by the ITU [32]. In

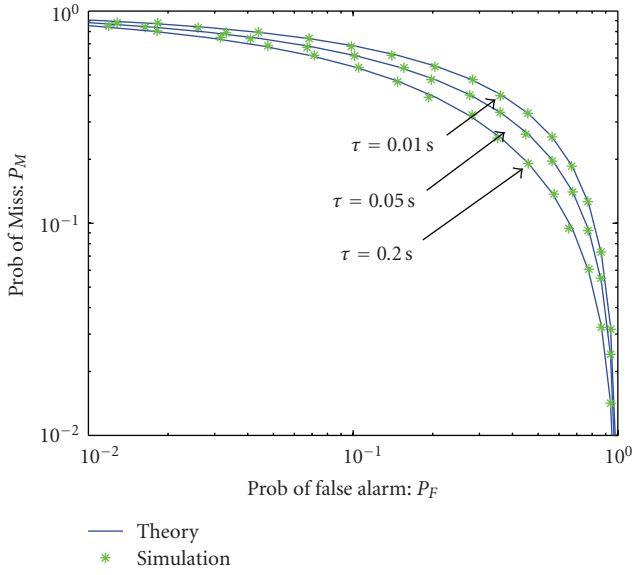

Figure 9: Complementary receiver operating characteristics curves for various holding times for the envelope based detector with $W = 7$ GHz, $B_w = 500$ MHz, $T_w = 0.7$ sec, $f_1 = 3.5$ GHz, $\lambda = 15\,(\text{sec}^{-1})$, $\gamma = 5$ dB.

[28], the exponential model is also verified experimentally for aggregated HSDPA data traffic by Telefonica I + D. Based on the type of traffic, the exponential model can also be extended to obtain further traffic models such as Erlange and Phase-type models [32]. However, in our paper, we adopt the exponential model whereas the other models could simply follow similar analytical procedures. We also adopt another model for the random hold time which suits modern teletraffic such as the World Wide Web IP traffic, namely, the Pareto distributed hold time model. The Pareto model is (experimentally) proven to fit Internet traffic as described in [28, 37, 53–56]. Furthermore, in practice, the analyses for the constant τ with the M/D/1 model and the random τ with exponential and Pareto models are all useful depending on the type of traffic generated by the PU.

The exponentially distributed hold time τ is given by the density function $f_\tau(\tau) = 1/\tau_a \exp(-\tau/\tau_a)$, with a mean hold time of τ_a. The Pareto distributed hold time τ is given by the density function $f_\tau(\tau) = k\tau_{\min}^k \tau^{-(k+1)}$ for $\tau > \tau_{\min}$ and $\forall k > 0$, with $E[\tau] = \tau_b = k\tau_{\min}/(k-1)$ for $k > 1$ and $E[(\tau - \tau_b)^2] = k\tau_{\min}^2/[(k-1)^2(k-2)]$ for $k > 2$. The parameter k for the Pareto model describes the peaky nature of the density function and $\tau_{\min}$ describes the minimum hold time that models a typical IP packet oriented service.

8.1. Theoretical Analysis. Using the exponential and Pareto hold time models with Poisson arrival for the PU transmission we rederive the expression for the probability of detection here for random τ. The probability of false alarm P_F stays unchanged, as in (17), because P_F is independent of the transmission statistics of the PU (i.e., P_F is independent of τ). From (17), we derive the new probability of detection for the random hold time by averaging over all possible values of τ. Therefore, the probability of detection is given by

$$P_D = \int_0^\infty \left(\exp\left(-\frac{\mu^2}{2\sigma^2}\right) P'_M + Q_1\left(\frac{E_r}{\sigma}, \frac{\mu}{\sigma}\right) P'_D \right) f_\tau(\tau) d\tau. \tag{19}$$

(Note that for the Pareto model the integration range in the above is from $\tau_{\min}$ to ∞.) By solving the integral in (19) for both exponential and Pareto models, we come up with a closed form expression for P_D as

$$P_D = P''_M \left(\exp\left(-\frac{\mu^2}{2\sigma^2}\right) - Q_1\left(\frac{E_r}{\sigma}, \frac{\mu}{\sigma}\right) \right) + Q_1\left(\frac{E_r}{\sigma}, \frac{\mu}{\sigma}\right), \tag{20}$$

where $P''_M = \int_0^\infty P'_M f_\tau(\tau) d\tau$ is the probability of miss detection for the random τ in the absence of the sensing noise (i.e., considering only the transmission statistics of the PU), given by

$$P''_M = \begin{cases} \dfrac{\exp(-\lambda\Gamma)}{(1+\lambda\tau_a)} & \text{for the exponential model,} \\ \dfrac{k\exp(-\lambda(\tau_{\min}+\Gamma))}{(\lambda\tau_{\min}+k)} & \text{for the Pareto model.} \end{cases} \tag{21}$$

Furthermore, the probability of detection P''_D for random τ in the absence of noise is given by $P'_D(\tau) = 1 - P''_M$. The curves R_1 and R_2 defining the risk regions (Section 6) can also be redefined for the random holding time case. From Section 8.1 we have two new curves for the exponential hold time model given by

$$\begin{aligned} R_1^\tau &\Longrightarrow \ln\left(1 - P'_{D^L}\right) + \ln(1+\lambda\tau_a) + \lambda\Gamma = 0, \\ R_2^\tau &\Longrightarrow \ln\left(1 - P'_{D^H}\right) + \ln(1+\lambda\tau_a) + \lambda\Gamma = 0. \end{aligned} \tag{22}$$

The new curves in (22) differ mainly for low values of λ but has the same limit values of Δ_a^L and Δ_a^H defining the risk regions, as in (15), when $\tau_a \to 0$.

8.2. Numerical Results. We compare the differences in the detection performance between the constant τ and the random τ cases. The random τ case obviously relates to reality more than the former. Figure 10 depicts the theoretical curves for the probability of miss detection with respect to the arrival rate λ for the noiseless case. The figure shows both the constant and the random τ cases for the exponential and the Pareto models. As we observe from the figure, the differences between the two arise for higher values of mean hold time and λ. This is due to the fact that for larger values of τ_a and τ_b, the probability of having smaller hold times is greater in the random case, and hence we observe poorer performances compared to the constant τ case. Figure 11 on the other hand shows the complementary ROC curves for the random and constant τ cases for noisy sensing. In Figure 10, we observed that the differences between the random and the

constant τ detection performances arise for higher values of (both) mean hold time and λ, and in Figure 11 we observe that the difference between the two arise only when the SNR is higher, provided that the mean hold time and λ are high. For lower values of γ we see that the difference is negligible. Furthermore, we observe that Pareto model shows better detection performance compared to the exponential model based on the value of $k(=2)$ for the same mean hold time. Note that when k increases the, Pareto model approaches the constant hold time case because the density function gets more peakier.

9. Minimum Required Spectrum Sensing Time

The temporal behavior of the PU influences the required spectrum sensing time for the CR node to reliably detect the PU. From the theoretical analyses performed in the previous sections, we study the minimum required sensing time to reliably detect the narrow band PU by a wideband CR node with a given confidence level. We compute the minimum required time for spectrum sensing based (only) on the temporal characteristics of the PU for both constant and random τ cases. The advantages of knowing the minimum required sensing time $T_w = T_w^{\min}$ here is two fold, (1) To reliably detect the PU with a given confidence level by not underscanning the spectrum (not scanning lower than the minimum required time) and (2) To save power at the CR node by not overscanning the spectrum (not scanning higher than the minimum required time), From (9) and Section 8.1, for a given confidence level of Υ% (i.e., probability of detection is Υ) for detecting the PU, the minimum required spectrum sensing time $T_w^{\min}$ for the constant and random hold time τ cases are given by

$$\begin{aligned} T_w \geq T_w^{\min} &= -\frac{W\ln(1-\Upsilon)}{B_w\lambda} \\ &\quad -\frac{W\tau}{B_w} \Longrightarrow \text{for constant } \tau, \\ T_w \geq T_w^{\min} &= -\frac{W\ln[(1-\Upsilon)(1+\lambda\tau_a)]}{B_W\lambda} \\ &\quad \Longrightarrow \text{for random exponential } \tau, \\ T_w \geq T_w^{\min} &= -\frac{W\ln[(1/k)(1-\Upsilon)(\lambda\tau_{\min}+k)]}{B_W\lambda} \\ &\quad -\frac{W\tau_{\min}}{B_w} \Longrightarrow \text{for random Pareto } \tau. \end{aligned} \tag{23}$$

The expressions in (23) can then be used by the CR nodes to dynamically adopt the spectrum sensing time T_w, given the hardware capability to adopt its time to sense, to reliably detect the PU, and at the same time save power. The temporal characteristics of the PU that is required to compute $T_w^{\min}$ may be known a priori or be acquired by learning the environment at the CR node.

Example 2 (Minimum Sensing Time for WiMedia-UWB CR node for Detecting WiMax). In this section we provide an example, continuing form Example 1 in Section 6, for a WiMedia-UWB based CR to detect a WiMax terminal with 90% confidence and the minimum required time to sense the spectrum. Note that, again here we assume as explained in Example 1 that the WiMax transmission has a Poisson arrival process.

Figure 12 shows the curves of $T_w^{\min}B_w/W$ for 90% confidence in detecting the PU for both constant and random

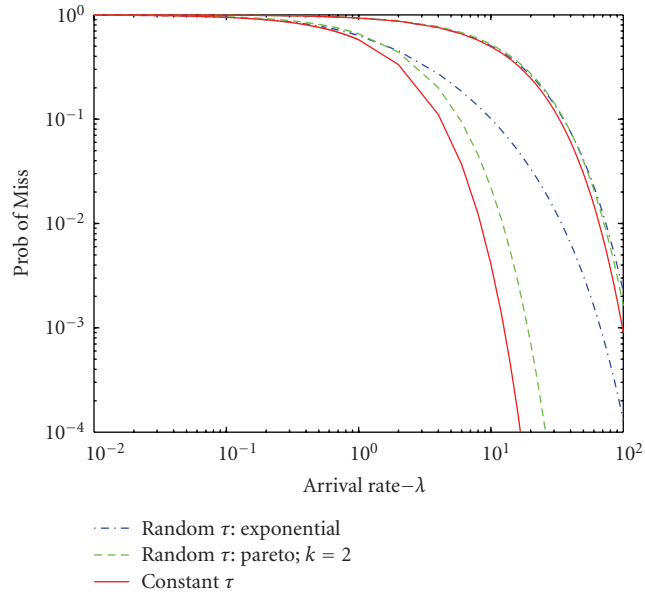

Figure 10: Probability of miss detection for the noiseless case with constant τ and random exponentially distributed τ, for $W = 7$ GHz, $B_w = 500$ MHz, $T_w = 0.7$ sec, $f_1 = 3.5$ GHz.

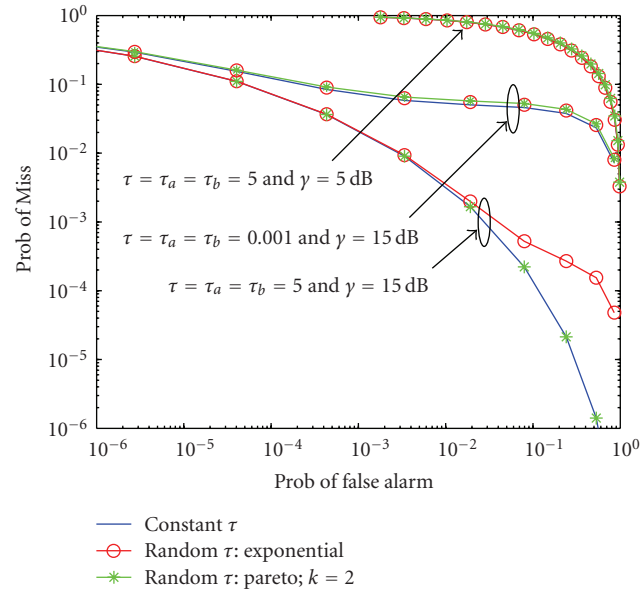

Figure 11: Complementary ROC curves with constant τ and random exponentially distributed τ, for $W = 7$ GHz, $B_w = 500$ MHz, $T_w = 0.7$ sec, $f_1 = 3.5$ GHz, $\lambda = 50$: Note: The τ values specified in the figure are for the constant hold time case, and τ_a values are for the random hold time case.

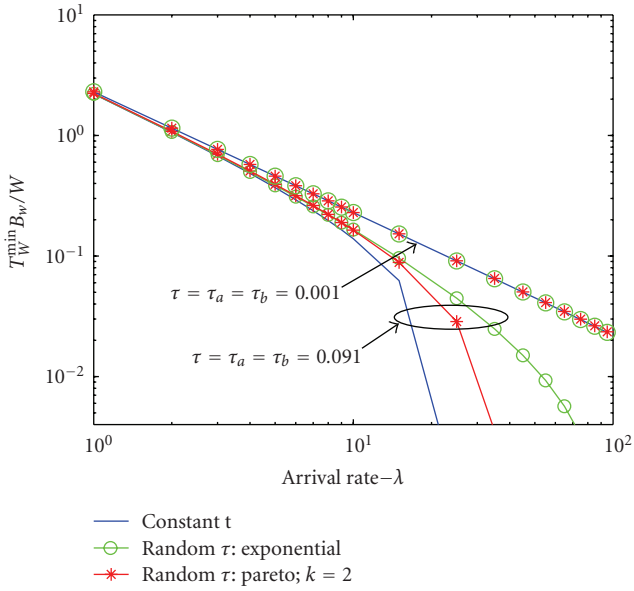

FIGURE 12: Duration of the spectrum sensing time (T_w) requirement for 90% confidence in detecting the PU, based on the temporal characteristics of the PU, with $W = 1.5$ GHz, $B_w = 10$ MHz.

τ considering only the SoS of the PU (without noise). The figure shows the curves with respect to the arrival rate λ for various values of mean hold times. From the results; we observe that the minimum time required to sense the spectrum increases when the arrival rate (λ) is low and as well as when the holding time is low. In the figure, we also show the operational region (for $T_w > T_w^{\min}$) and the inoperational region (for $T_w < T_w^{\min}$) of the CR nodes to reliably detect the PU (in the absence of noise). We further observe from the figure that the minimum sensing time $T_w^{\min}$ reduces significantly when the hold time increases. Though the results shown in Figure 12 is for the noiseless case, it holds true for relatively high values of γ. Similar analytical curves also can be generated for the noisy case by following the above procedure.

10. Conclusion

In this paper, we presented some detailed theoretical analysis on the performance of detecting a narrow band PU by a wideband CR terminal. The performance analyses were based on noisy sensing at the CR node as well as on the temporal characteristics of the PU. Closed form expressions were presented for the probabilities of detection, miss detection, and false alarm at the CR node, and were also verified using simulations. Further, we classify different risk regions for miss detecting the PU based on the temporal characteristics of the PU transmission, and consequently derive the minimum required spectrum sensing time to reliably detect the PU with a given confidence level. The analyses and the results were presented for both constant and random spectrum holding time, as well as random spectrum idle time considering the Poisson arrival process. Further research is to be conducted for optimizing the detection threshold for envelope- (energy-) based detection depending on the temporal characteristics of the PU together with the sensing noise. From the analytical framework that is provided in this paper, application (traffic) specific temporal (empirical) model for PU transmissions can also be used to perform similar analysis.

Acknowledgments

The research work was partly funded through the EU-FP7 Grant FP7-ICT-215669 under the EUWB Integrated Project. The authors would like to thank Professor Stephen Hanly from the University of Melbourne for his valuable comments.

References

[1] J. Mitola III and G. Q. Maguire Jr., "Cognitive radio: making software radios more personal," *IEEE Personal Communications*, vol. 6, no. 4, pp. 13–18, 1999.

[2] S. Haykin, "Cognitive radio: brain-empowered wireless communications," *IEEE Journal on Selected Areas in Communications*, vol. 23, no. 2, pp. 201–220, 2005.

[3] H. Arslan, Ed., *Cognitive Radio, Software Defined Radio, and Adaptive Wireless Systems*, Springer, Dordrecht, The Netherlands, 2007.

[4] E. Hossain and V. Bhargava, Eds., *Cognitive Wireless Communication Networks*, Springer, New York, NY, USA, 2007.

[5] "Federal Communications Commission, Facilitating Opportunities for Flexible, Efficient, and Reliable Spectrum Use Employing Cognitive Radio Technologies, NPRM and Order," ET Docket no. 03-322, December 2003.

[6] "The Commission of the European Communities, Commission Decision 2007/131/EC on allowing the use of the radio spectrum for equipment using ultra-wideband technology in a harmonised manner in the Community," Official Journal of the European Union, February 2007.

[7] G. Heidari, *WiMedia UWB: Technology of Choice for Wireless USB and Bluetooth*, John Wiley & Sons, New York, NY, USA, 2006.

[8] EUWB consortium, http://www.euwb.eu/.

[9] S. Kandeepan, et al., "D2.1.1:Spectrum Sensing and Monitoring," EUWB Integrated Project, European Commissiona Funded Project EC: FP7-ICT-215669, May 2009, http://www.euwb.eu/.

[10] D. Cabric, S. M. Mishra, and R. W. Brodersen, "Implementation issues in spectrum sensing for cognitive radios," in *Proceedings of the 38th Asilomar Conference on Signals, Systems and Computers*, vol. 1, pp. 772–776, Pacific Grove, Calif, USA, November 2004.

[11] A. Sahai, N. Hoven, and R. Tandra, "Some fundamental limits on cognitive radio," in *Proceedings of the 42nd Allerton Conference on Communication, Control and Computing*, Monticello, Minn, USA, September 2004.

[12] D. B. Cabric, *Cognitive Radios: System Design Perspective*, Ph.D. thesis, University of California, Berkeley, Calif, USA, 2007.

[13] P. Wang, L. Xiao, S. Zhou, and J. Wang, "Optimization of detection time for channel efficiency in cognitive radio systems," in *Proceedings of IEEE Wireless Communications and Networking Conference (WCNC '07)*, pp. 111–115, Kowloon, Hong Kong, March 2007.

[14] G. Amir and S. S. Elvino, "Opportunistic spectrum access in fading channels through collaborative sensing," *Journal on Communications*, vol. 2, no. 2, pp. 71–82, 2007.

[15] Z. Quan, S. Cui, A. H. Sayed, and H. V. Poor, "Wideband spectrum sensing in cognitive radio networks," in *Proceedings of the IEEE International Conference on Communications (ICC '08)*, pp. 901–906, Beijing, China, May 2008.

[16] W.-Y. Lee and I. F. Akyildiz, "Optimal spectrum sensing framework for cognitive radio networks," *IEEE Transactions on Wireless Communications*, vol. 7, no. 10, pp. 3845–3857, 2008.

[17] D. Cabric, A. Tkachenko, and R. W. Brodersen, "Experimental study of spectrum sensing based on energy detection and network cooperation," in *Proceedings of the 1st International ACM Workshop on Technology and Policy for Accessing Spectrum*, Boston, Mass, USA, 2006.

[18] T. C. Aysal, S. Kandeepan, and R. Piesiewicz, "Cooperative spectrum sensing over imperfect channels," in *Proceedings of IEEE Globecom Workshops (GLOBECOM '08)*, New Orleans, La, USA, November-December 2008.

[19] T. C. Aysal, S. Kandeepan, and R. Piesiewicz, "Cooperative spectrum sensing with noisy hard decision transmissions," in *Proceedings of the IEEE International Conference on Communications (ICC '09)*, Dresden, Germany, June 2009.

[20] M. P. Wylie-Green, "Dynamic spectrum sensing by multiband OFDM radio for interference mitigation," in *Proceedings of the 1st IEEE International Symposium on New Frontiers in Dynamic Spectrum Access Networks (DySPAN '05)*, pp. 619–625, Baltimore, Md, USA, November 2005.

[21] M. M. Rashid, Md. J. Hossain, E. Hossain, and V. K. Bhargava, "Opportunistic spectrum access in cognitive radio networks: a queueing analytic model and admission controller design," in *Proceedings of the 50th Annual IEEE Global Telecommunications Conference (GLOBECOM '07)*, pp. 4647–4652, Washington, DC, USA, November 2007.

[22] Y. Pei, A. T. Hoang, and Y.-C. Liang, "Sensing-throughput tradeoff in cognitive radio networks: how frequently should spectrum sensing be carried out?" in *Proceedings of the 18th Annual IEEE International Symposium on Personal, Indoor and Mobile Radio Communications (PIMRC '07)*, Athens, Greece, September 2007.

[23] J. Ma and Y. Li, "A probability-based spectrum sensing scheme for cognitive radio," in *Proceedings of IEEE International Conference on Communications (ICC '08)*, pp. 3416–3420, Beijing, China, May 2008.

[24] S. Tang and B. L. Mark, "An adaptive spectrum detection mechanism for cognitive radio networks in dynamic traffic environments," in *Proceedings of IEEE Global Telecommunications Conference (GLOBECOM '08)*, pp. 3009–3013, New Orleans, La, USA, November-December 2008.

[25] X. Zhou, Y. Li, Y. H. Kwon, and A. C. K. Soong, "Detection timing and channel selection for periodic spectrum sensing in cognitive radio," in *Proceedings of IEEE Global Telecommunications Conference (GLOBECOM '08)*, pp. 2988–2992, New Orleans, La, USA, November-December 2008.

[26] S. Kandeepan, A. B. Rahim, T. C. Aysal, and R. Piesiewicz, "Time divisional and time-frequency divisional cooperative spectrum sensing," in *Proceedings of the 4th International Conference on Cognitive Radio Oriented Wireless Networks and Communications (CROWNCOM '09)*, Hannover, Germany, June 2009.

[27] S. Kandeepan, A. Giorgetti, and M. Chiani, "Time-divisional cooperative periodic spectrum sensing for cognitive radio networks," in *Proceedings of IEEE International Conference on Communications (ICC '10)*, Cape Town, South Africa, May 2010.

[28] S. Kandeepan, A. Sierra, J. Campos, and I. Chlamtac, "Periodic sensing in cognitive radios for detecting UMTS/HSDPA based on experimental spectral occupancy statistics," in *Proceedings of IEEE Wireless Communications & Networking Conference (WCNC '10)*, Sydney, Australia, April 2010.

[29] B. Jabbari, "Teletraffic aspects of evolving and next-generation wireless communication networks," *IEEE Personal Communications*, vol. 3, no. 6, pp. 4–9, 1996.

[30] T. Janevski, *Traffic Analysis and Design of Wireless IP Networks*, Artech House, Boston, Mass, USA, 2003.

[31] A. O. Allen, *Probability Statistics, and Queuing Theory with Computer Science Applications*, Academic Press, 1990.

[32] ITU Handbook, "Teletraffic Engineering, ITU-D," Study Group 2, June 2006, http://www.itu.int/.

[33] C. Park, H. Shen, F. Hernndez-Campos, J. S. Marron, and D. Veitch, "Capturing the elusive poissonity in web traffic," in *Proceedings of the 14th IEEE International Symposium on Modeling, Analysis, and Simulation of Computer and Telecommunication Systems (MASCOTS '06)*, pp. 189–196, Monterey, Calif, USA, September 2006.

[34] J. Cao, W. S. Cleveland, D. Lin, and D. X. Sun, "Internet traffic tends toward poisson and independent as the load increases," in *Nonlinear Estimation and Classification*, D. D. Denison, M. H. Hansen, C. C. Holmes, B. Mallick, and B. Yu, Eds., vol. 171 of *Lecture Notes in Statistics*, Springer, New York, NY, USA, 2003.

[35] P. Salvador, A. Pacheco, and R. Valadas, "Modeling IP traffic: joint characterization of packet arrivals and packet sizes using BMAPs," *Computer Networks*, vol. 44, no. 3, pp. 335–352, 2004.

[36] M. Mandjes, R. Van de Meent, and S. N. Quija, "Measuring modeling and cost allocation (M2C) project deliverable D2.1: a classification of IP traffic models," Project Report, December 2003, http://arch.cs.utwente.nl/projects/m2c/.

[37] M. Zukerman, T. D. Neame, and R. G. Addie, "Internet traffic modeling and future technology implications," in *Proceedings of the 22nd Annual Joint Conference on the IEEE Computer and Communications Societies*, vol. 1, pp. 587–596, San Francisco, Calif, USA, March-April 2003.

[38] T. Karagiannis, M. Molle, M. Faloutsos, and A. Broido, "A nonstationary poisson view of internet traffic," in *Proceedings of the 23rd Annual Joint Conference of the IEEE Computer and Communications Societies*, vol. 3, pp. 1558–1569, Hong Kong, March 2004.

[39] M. M. Krunz and A. M. Makowski, "Modeling video traffic using M/G/∞ input processes: a compromise between Markovian and LRD models," *IEEE Journal on Selected Areas in Communications*, vol. 16, no. 5, pp. 733–748, 1998.

[40] T. D. Neame, M. Zukerman, and R. G. Addie, "Modeling broadband traffic streams," in *Proceedings of the IEEE Global Telecommunication Conference (GLOBECOM '99)*, vol. 1, Rio de Janeiro, Brazil, December 1999.

[41] Y. Fang, I. Chlamtac, and Y.-B. Lin, "Modeling PCS networks under general call holding time and cell residence time distributions," *IEEE/ACM Transactions on Networking*, vol. 5, no. 6, pp. 893–906, 1997.

[42] B. A. Mah, "Empirical model of HTTP network traffic," in *Proceedings of the 16th IEEE Annual Conference on Computer Communications (INFOCOM '97)*, vol. 2, pp. 592–600, Kobe, Japan, April 1997.

[43] V. A. Bolotin, "Modeling call holding time distributions for CCS network design and performance analysis," *IEEE Journal on Selected Areas in Communications*, vol. 12, no. 3, pp. 433–438, 1994.

[44] F. Barcelo and S. Bueno, "Idle and inter-arrival time statistics in public access mobile radio (PAMR) systems," in *Proceedings of the IEEE Global Telecommunications Conference*, vol. 1, pp. 126–130, Phoenix, Ariz, USA, November 1997.

[45] H. Urkowitz, "Energy detection of unknown deterministic signals," *Proceedings of the IEEE*, vol. 55, no. 4, pp. 523–531, 1967.

[46] S. Kay, *Intuitive Probability and Random Processes Using Matlab*, Springer, New York, NY, USA, 2006.

[47] M. Wellens, A. de Baynast, and P. Mähönen, "Performance of dynamic spectrum access based on spectrum occupancy statistics," *IET Communications*, vol. 2, no. 6, pp. 772–782, 2008.

[48] T. Kailath and H. Vincent Poor, "Detection of stochastic processes," *IEEE Transactions on Information Theory*, vol. 44, no. 6, pp. 2230–2259, 1998.

[49] R. Tandra and A. Sahai, "Fundamental limits on detection in low SNR under noise uncertainty," in *Proceedings of International Conference on Wireless Networks, Communications and Mobile Computing*, vol. 1, pp. 464–469, Maui, Hawaii, USA, June 2005.

[50] F. F. Digham, M.-S. Alouini, and M. K. Simon, "On the energy detection of unknown signals over fading channels," *IEEE Transactions on Communications*, vol. 55, no. 1, pp. 21–24, 2007.

[51] T. S. Rappaport, *Wireless Communications: Principles and Practice*, Prentice Hall, Upper Saddle River, NJ, USA, 2nd edition, 2002.

[52] J. G. Andrews, A. Ghsoh, and R. Muhamed, *Fundamentals of WiMAX: Understanding Braodband Wireless Networking*, Prentice Hall, Upper Saddle River, NJ, USA, 2007.

[53] M. E. Crovella and A. Bestavros, "Self-similarity in world wide web traffic evidence and possible causes," *Performance Evaluation Review*, vol. 24, no. 1, pp. 160–169, 1996.

[54] K. Park, G. Kim, and M. Crovella, "On the relationship between file sizes, transport protocols, and self-similar network traffic," in *Proceedings of the International Conference on Network Protocols*, pp. 171–180, Columbus, Ohio, USA, October-November 1996.

[55] W. Willinger, M. S. Taqqu, R. Sherman, and D. V. Wilson, "Self-similarity through high-variability: statistical analysis of Ethernet LAN traffic at the source level," *IEEE/ACM Transactions on Networking*, vol. 5, no. 1, pp. 71–86, 1997.

[56] R. G. Addie, T. D. Neame, and M. Zukerman, "Modeling superposition of many sources generating self similar traffic," in *Proceedings of IEEE International Conference on Communications (ICC '99)*, vol. 1, pp. 387–391, Vancouver, Canada, June 1999.